J Physiol 596.12 (2018) pp 2447–2461

The Journal of Physiology

Synaptic depression induced by postsynaptic cAMP production in the *Drosophila* mushroom body calyx

Shoma Sato[1], Kohei Ueno[2], Minoru Saitoe[2] and Takaomi Sakai[1]

[1] *Department of Biological Sciences, Tokyo Metropolitan University, 1-1 Minami-osawa, Hachioji, Tokyo, 1920372, Japan*
[2] *Learning and Memory Project, Tokyo Metropolitan Institute of Medical Science, 2-1-6 Kamikitazawa, Setagaya-ku, Tokyo, 1568506, Japan*

Edited by: Ian Forsythe & Reinhold Penner

Key points

- Synaptic potentiation in *Drosophila* is observed at cholinergic synapses between antennal lobe (AL) and mushroom body (MB) neurons in the adult brain; however, depression at the AL–MB synapses has not yet been identified.
- By *ex vivo* Ca^{2+} imaging in an isolated cultured *Drosophila* brain, we found novel activity-dependent depression at the AL–MB synapses.
- The degree of Ca^{2+} responses after repetitive AL stimulation is significantly reduced in the dendritic region of MB neurons (calyx) compared with those before AL stimulation, and this reduction of Ca^{2+} responses remains for at least 30 min.
- The expression of *rutabaga*, which encodes Ca^{2+}/calmodulin-dependent adenylyl cyclase, is essential in the MB neurons for the reduction of Ca^{2+} responses in the calyx.
- Our study reveals that elevation of cAMP production in the calyx during repetitive AL stimulation induces the depression at the AL–MB synapses.

Abstract Synaptic plasticity has been studied to reveal the molecular and cellular mechanisms of associative and non-associative learning. The fruit fly *Drosophila melanogaster* can be used to identify the molecular mechanisms of synaptic plasticity because vast genetic information or tools are available. Here, by *ex vivo* Ca^{2+} imaging of an isolated cultured *Drosophila* brain, we examined the novel activity-dependent synaptic depression between the projection neurons of the antennal lobe (AL) and mushroom body (MB). *Ex vivo* Ca^{2+} imaging analysis revealed that electrical stimulation of AL elicits Ca^{2+} responses in the dendritic (calyx) and axonal (α lobe) regions of MB neurons, and the responses are reduced after repetitive AL stimulation. Since the cAMP signalling pathway plays an important role in synaptic plasticity in invertebrates and vertebrates, we examined whether the reduction of Ca^{2+} responses is also regulated by the cAMP signalling pathway. The expression of *rutabaga* (*rut*), which encodes Ca^{2+}/calmodulin-dependent adenylyl cyclase, was essential for the reduction of Ca^{2+} responses in the calyx and α lobe. Furthermore,

Shoma Sato is a PhD candidate in the Department of Biological Sciences at Tokyo Metropolitan University. His research interests are on the molecular and cellular mechanisms of neural plasticity underlying memory formation.

DOI: 10.1113/JP275799

imaging analysis using a fluorescence resonance energy transfer-based cAMP indicator revealed that the cAMP level increased in the wild-type calyx during repetitive AL stimulation, whereas it decreased in *rut*^{1} mutant flies with a loss-of-function mutation of *rut*. Thus, our study suggests that an increase in postsynaptic cAMP level during repetitive AL stimulation contributes to the attenuation of inputs at AL–MB synapses.

(Resubmitted 15 March 2018; accepted after revision 6 April 2018; first published online 25 April 2018)
Corresponding author T. Sakai: Department of Biological Sciences, Tokyo Metropolitan University, 1-1 Minami-osawa, Hachioji, Tokyo 1920372, Japan. Email: sakai-takaomi@tmu.ac.jp

Introduction

In invertebrates and vertebrates, synaptic plasticity has been extensively studied to reveal the possible molecular and cellular mechanisms of memory formation (Kandel, 2001; Ho *et al.* 2011). The repetitive stimulation of single-target neurons or the paired associative stimulation of multiple-target neurons can enhance or weaken synaptic efficacy leading to long-term potentiation (LTP) and long-term depression (LTD) (Collingridge *et al.* 2010; Nicoll, 2017). It has been considered that LTP and LTD underlie some forms of memory in *Aplysia* or mice (Hawkins *et al.* 2006; Glanzman, 2009; Korte & Schmitz, 2016). The cAMP signalling pathway plays an important role in memory formation and synaptic plasticity, in invertebrates and vertebrates (Abel & Nguyen, 2008; Kandel, 2012). Thus, the significance of cAMP signalling in behavioural and synaptic plasticities may be evolutionarily conserved across species.

The fruit fly *Drosophila melanogaster* has been used as a model to identify the molecular mechanisms of synaptic plasticity because vast genetic information or tools are available. The *Drosophila* mushroom bodies (MBs) are critical brain structures for associative and non-associative olfactory memory (Heisenberg, 2003; Cho *et al.* 2004). The dendritic region of MB neurons (calyx) receives olfactory information through cholinergic inputs from the projection neurons (PNs) of the antennal lobe (AL) (Vosshall & Stocker, 2007), where each MB neuron extends to three types of axonal lobe (α/β, α'/β' and γ lobes) (Crittenden *et al.* 1998), and MB axons innervate individual MB output neurons (MBONs) (Aso *et al.* 2014). Some genes associated with the cAMP signalling pathway are expressed in MB neurons (e.g. *rutabaga* (*rut*), encoding an adenylyl cyclase (AC), and *dunce* (*dnc*), encoding a phosphodiesterase) (Davis, 2005). Thus, it is possible that the cAMP signalling pathway is also involved in the regulation of the synaptic plasticity of MB neurons.

In *Drosophila*, *in vivo* Ca^{2+} imaging of brain activity revealed that odour-evoked Ca^{2+} responses in MB lobes were enhanced after association between the odour and an electrical shock (Davis, 2011). Furthermore, *ex vivo* Ca^{2+} imaging using an isolated cultured *Drosophila* brain is also a powerful tool to identify physiological properties related to synaptic plasticity in specific brain neurons (Wang *et al.* 2008; Ueno *et al.* 2013; Cohn *et al.* 2015). Similar to mammalian LTP, synaptic potentiation in *Drosophila*, also known as long-term enhancement (LTE), is observed in synapses between AL and MB neurons. Ca^{2+} responses in the MB neurons induced by AL stimulation are enhanced after the simultaneous associative stimulation of the AL and the ascending fibres of the ventral nerve cord (AFV) in an isolated cultured *Drosophila* brain (Ueno *et al.* 2013). In contrast to LTE in the fly brain, at the *Drosophila* larval neuromuscular junction, synaptic depression can be induced by specific patterns of tetanic stimulation in a cAMP-independent manner (Guo & Zhong, 2006). In addition, in the fly brain, pairing an odour with the activation of specific dopaminergic neurons induces the synaptic depression of MBON inputs (Hige *et al.* 2015), although the molecular mechanisms regulating this synaptic depression remain unclarified.

In this study, by non-associative repetitive stimulation, we examined the novel synaptic depression in an isolated cultured *Drosophila* brain. We identified that Ca^{2+} responses in the MB calyx and α lobe induced by AL stimulation are reduced after repetitive AL stimulation. The reduction of Ca^{2+} responses remained for at least 30 min after the repetitive AL stimulation. In addition, we examined whether the presynaptic or postsynaptic cAMP signalling modulates the reduction of Ca^{2+} responses after the repetitive AL stimulation.

Methods

Fly stocks

Fly stocks used for this study are as follows: *rut*^{1}, *dnc*^{1}, GH146 (Bloomington Drosophila Stock Center (BS), Bloomington, IN, USA, no. 30026), MB-GAL4 lines (MB247, c305a, c772, R13F02-GAL4 (BS, no. 48571) and 30Y), MB-LexA (II), MB-LexA (III) (Ueno *et al.* 2013), UAS-*GCaMP3* (BS, no. 32236), UAS-*GCaMP6m* (BS, no. 42748), UAS-*Epac1-camps* (BS, no. 25408), UAS-*rut* (BS, no. 9405), LexAop-*GCaMP6f* (BS, no. 44277)

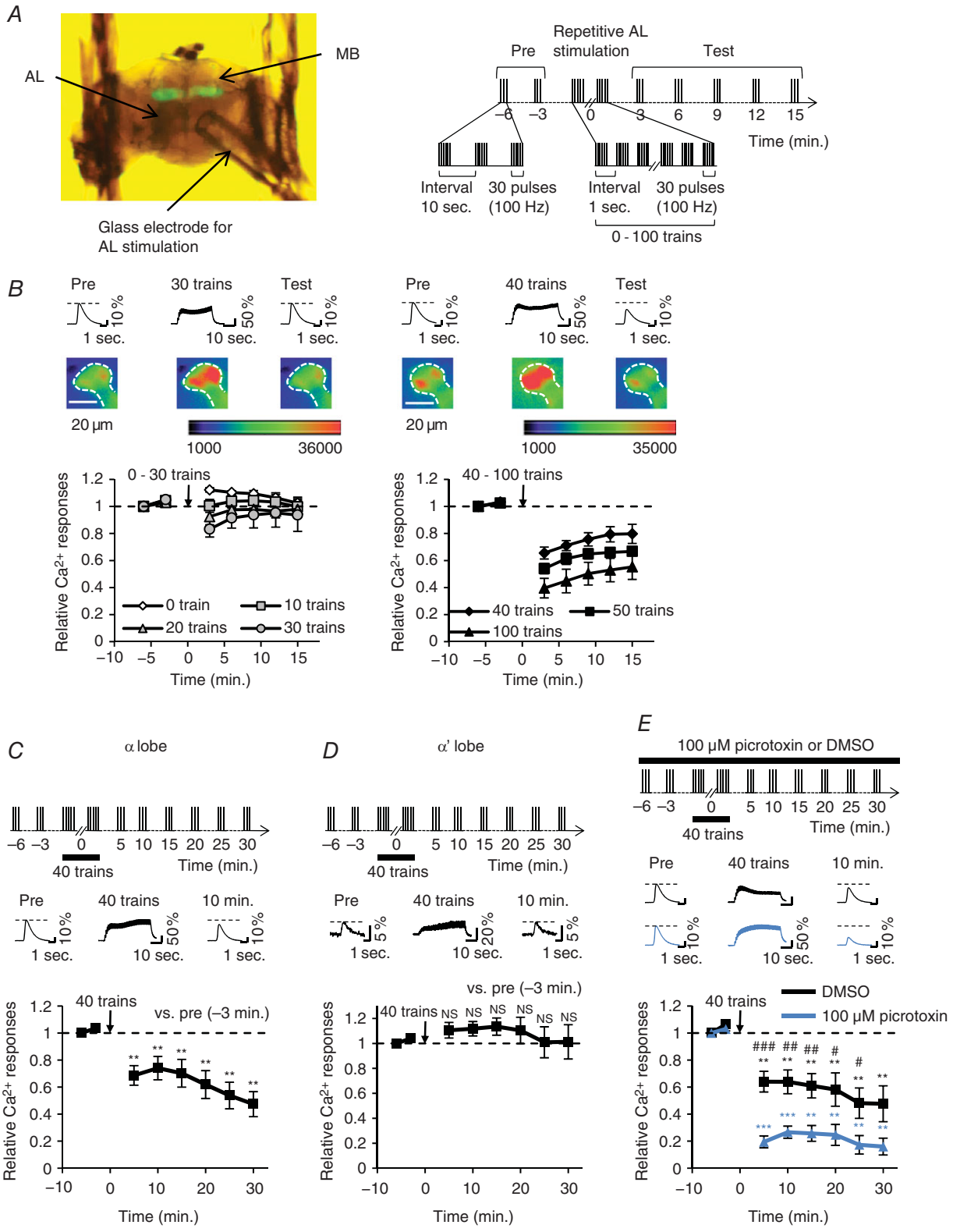

Figure 1. Repetitive AL stimulation induces the reduction of Ca^{2+} responses in the MB α lobe

A–C and *E*, +; MB247 UAS-*GCaMP3*/+ males were used in the experiments. *A*, the left image shows a brain preparation for experiments. A schematic diagram of the stimulation protocol is shown on the right. A glass microelectrode was attached onto the AL. AL was stimulated at 3 min intervals. *B*, relative Ca^{2+} responses before and after repetitive AL stimulation. $n = 6$–8 brains in each train. The upper panels show typical Ca^{2+} responses in the α lobe tip 3 min before (Pre), during and 9 min after (Test) repetitive AL stimulation. Number of trains in repetitive AL stimulation were 30 (left panels) and 40 (right panels). Pseudo-color represents the intensity of GCaMP3 fluorescence. The area indicated by dotted lines is the α lobe tip. *C*, Ca^{2+} responses before and after application of 40 stimulus trains in the α lobe tip. The upper panel shows a schematic diagram of the stimulation protocol. AL stimulation was applied sequentially every 3 min before the application of 40 stimulus trains. Subsequently, AL stimulation was applied every 5 min after the application of 40 stimulus trains. The middle panel shows typical Ca^{2+} responses in the α lobe tip 3 min before (Pre), during and 10 min after the application of 40 stimulus trains. Asterisks indicate the statistical significance of difference at each time point between before and after the application of 40 stimulus trains. The Mann–Whitney *U* test was used for statistical analysis. Error bars represent SEM. $^{**}P < 0.01$; $n = 7$. *D*, c305a/+; UAS-*GCaMP3*/+ males were used. Ca^{2+} responses before and after application of 40 stimulus trains in the α' lobe tip. The upper panel shows a schematic diagram of the stimulation protocol. The middle panel shows typical Ca^{2+} responses in the α' lobe tip 3 min before (Pre), during and 10 min after the application of 40 stimulus trains. No significant difference was detected at each time point between before and after the application of 40 stimulus trains. Student's *t* test or the Mann–Whitney *U* test was used for statistical analysis. Error bars represent SEM. NS, not significant; $n = 7$. *E*, $GABA_A$ receptor inhibition does not impair the reduction of Ca^{2+} responses. The upper panel shows a schematic diagram of the stimulation protocol. The middle panel shows typical Ca^{2+} responses in the α lobe tip 3 min before (Pre), during and 10 min after the application of 40 stimulus trains. The reduction of Ca^{2+} responses was enhanced by the treatment of the $GABA_A$ receptor blocker picrotoxin (blue line; $n = 6$) compared with that of DMSO as the control (black line; $n = 6$). Asterisks indicate the statistical significance of the difference between before and after the application of 40 stimulus trains. Hash symbols indicate the statistical significance of difference at each time point between picrotoxin treatment and DMSO control. Student's *t* test or the Mann–Whitney *U* test was used for statistical analysis. Error bars represent SEM. $^{**}P < 0.01$; $^{***}P < 0.001$; $^{\#}P < 0.05$; $^{\#\#}P < 0.01$; $^{\#\#\#}P < 0.001$. [Colour figure can be viewed at wileyonlinelibrary.com]

and LexAop-*GCaMP6m* (BS, no. 44275). Flies were raised on glucose–yeast–cornmeal medium at 25.0 ± 0.5°C in a 12 h light:12 h dark cycle. We used 1- to 2-day-old males in all experiments.

Brain preparation

Brains were prepared for imaging analysis as previously described with minor modifications (Ueno *et al.* 2013, 2017; Naganos *et al.* 2016). Briefly, brains were dissected in 0 mM Ca^{2+} HL3 medium (in mM, NaCl, 70; sucrose, 115; KCl, 5; $MgCl_2$, 20; $NaHCO_3$, 10; trehalose, 5; Hepes, 5; pH 7.3) (Stewart *et al.* 1994). As previously described, the isolated brains were immobilized by placing their optic lobes between two nylon fibre bundles attached to a platinum grid, and were placed in a recording chamber filled with normal HL3 medium (in mM: NaCl, 70; sucrose, 115; KCl, 5; $MgCl_2$, 20; $CaCl_2$, 1.8; $NaHCO_3$, 10; trehalose, 5; Hepes, 5; pH 7.3). During the experiments, fresh HL3 medium was infused into the chamber using a peristaltic pump (1–2 ml min^{-1}, AC-2110, ATTO Corporation, Tokyo, Japan) or a Pasteur pipette every 5–10 min.

Electrical stimulation

The AL was electrically stimulated using glass microelectrodes with a stimulator (SEN-8203 and SEN-7103, Nihon Kohden, Tokyo, Japan) and an isolator (SS-203J and SS-202J, Nihon Kohden). To record Ca^{2+} responses in the PNs or the MB calyx or lobes, we stimulated the AL with three trains of 30 pulses (100 Hz, 1.0 ms pulse duration, intensity 1–2 times threshold current (0.08–0.12 mA)) at intertrain intervals of 10 s. To apply repetitive AL stimulation, we stimulated the AL with 10–100 trains of 30 pulses (100 Hz, 1.0 ms pulse duration) at intertrain intervals of 1.0 s. The AL was stimulated sequentially before and after repetitive AL stimulation every 3 or 5 min.

Ca^{2+} imaging

For Ca^{2+} imaging using GCaMP3 or GCaMP6m, fluorescence images were captured at 30–32 Hz using a fluorescence microscope (ECLIPSE FN1, Nikon Corp., Tokyo, Japan) equipped with a 20× water-immersion objective (NA, 0.5; Nikon Corp.), and all recordings were captured using an electron multiplier CCD camera (QuantEM:512SC, Photometrics, Tucson, AZ, USA). GCaMP3 or GCaMP6m were excited at 455–485 nm and detected using a 500–545 nm band-pass filter. The intensity of fluorescence (F) values were calculated for all pixels in the region of interest using NIS-Elements AR software (Nikon Corp.). We calculated the initial F value (F_0) by averaging the F values recorded from 10 sequential frames before stimulation. To obtain $\Delta F/F_0$ (%) as Ca^{2+} responses, we calculated $(F - F_0)/F_0 \times 100$ in each time point. To measure AL stimulation-induced Ca^{2+} responses ($\Delta F/F_{0\ ave}$), we calculated the average $\Delta F/F_0$ change from

three AL stimulations. To calculate relative Ca^{2+} responses, $\Delta F/F_{0\ ave}$ in each time point was divided by $\Delta F/F_{0\ ave}$ at the first time point.

cAMP imaging

Epac1-camps was used for cAMP imaging. For the measurement of cAMP responses during repetitive AL stimulation, fluorescence images were captured at 1 Hz using a confocal microscope system (A1R, Nikon Corp.) equipped with a 20× water-immersion objective (NA, 0.5; Nikon Corp.). Cyan fluorescent protein (CFP) was excited at 458 nm and detected using a 482 ± 17.5 nm band-pass filter, and yellow fluorescent protein (YFP) was detected simultaneously using a 540 ± 15 nm band-pass filter. We calculated fluorescence resonance energy transfer (FRET) changes as R using the following formula: $R = F$ of CFP/F of YFP. We calculated the initial R (R_0) by averaging the R values recorded from 10 sequential frames before stimulation. To obtain $\Delta R/R_0$ (%) as cAMP responses, we calculated $(R - R_0)/R_0 \times 100$ in each time point.

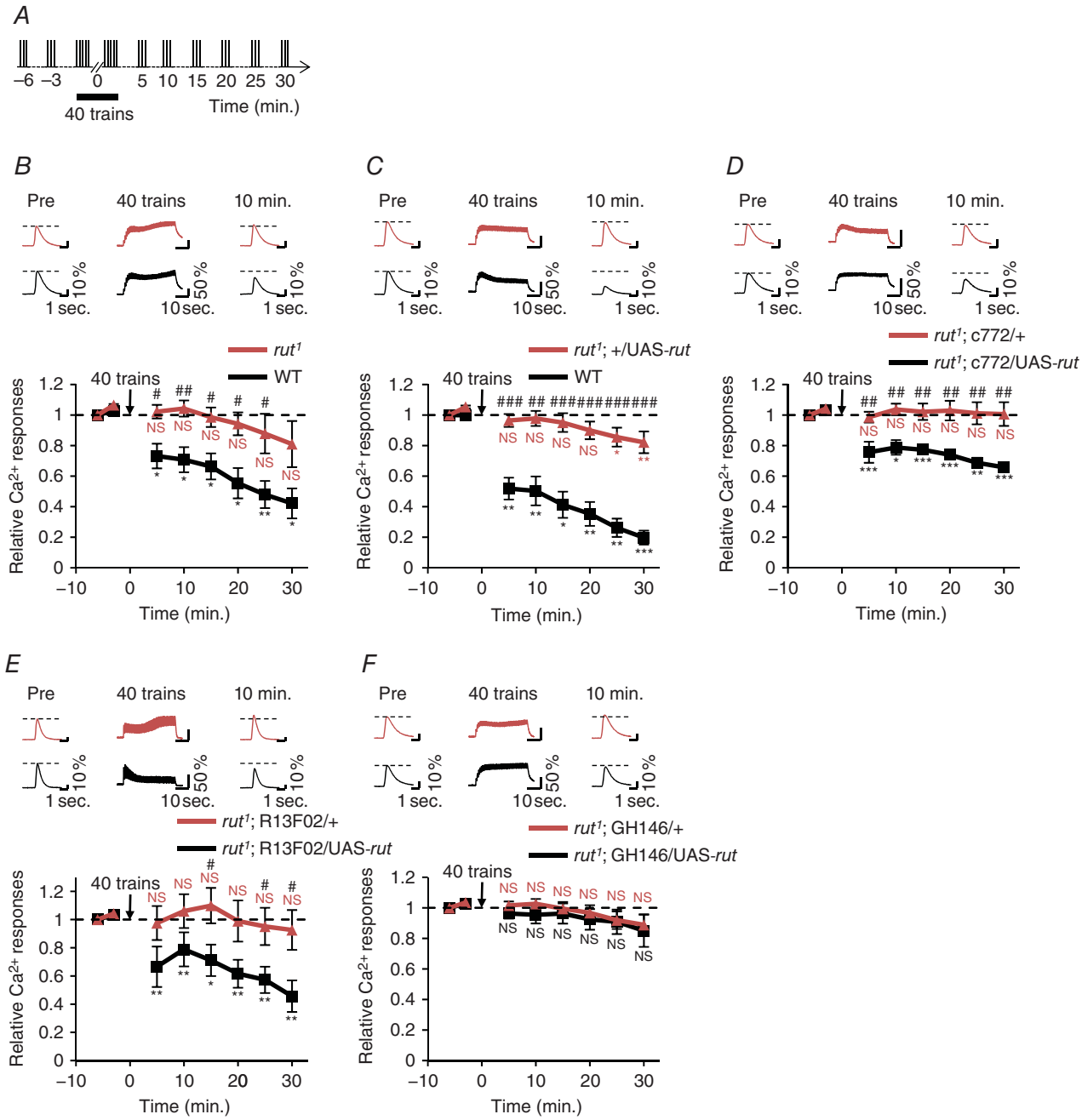

Figure 2. *rut* expression in MB neurons is required for the reduction of Ca^{2+} responses

A, schematic diagram of the stimulation protocol. *B–F*, the upper panels show typical Ca^{2+} responses in the α lobe tip 3 min before (Pre), during and 10 min after the application of 40 stimulus trains. Asterisks indicate the statistical significance of the difference between before and after the application of 40 stimulus trains. Student's *t* test or the Mann–Whitney *U* test was used for statistical analysis. Error bars represent SEM. NS, not significant; $^{*}P < 0.05$; $^{**}P < 0.01$; $^{***}P < 0.001$. *B*, relative Ca^{2+} responses in the wild-type (+; MB247 UAS-*GCaMP3*/+; $n = 6$; black line) and *rut*^{1} (*rut*^{1}; MB247 UAS-*GCaMP3*/+; $n = 6$, red line). Hash symbols indicate the statistical significance of difference at each time point between two genotypes. Student's *t* test was used for statistical analysis. $^{\#}P < 0.05$; $^{\#\#}P < 0.01$. *C*, relative Ca^{2+} responses in the wild-type (+; +; MB-LexA LexAop-*GCaMP6m*/+; $n = 5$; black line) and *rut*^{1} (*rut*^{1}; +/UAS-*rut*; MB-LexA LexAop-*GCaMP6m*/+; $n = 7$; red line). Hash symbols indicate the statistical significance of difference at each time point between two genotypes. Student's *t* test was used for statistical analysis. $^{\#\#}P < 0.01$; $^{\#\#\#}P < 0.001$. *D*, relative Ca^{2+} responses in *rut*^{1}; c772/UAS-*rut*; MB-LexA LexAop-*GCaMP6m*/+ (black line; $n = 7$) and *rut*^{1}; c772/+; MB-LexA LexAop-*GCaMP6m*/+ (red line; $n = 6$). Hash symbols indicate the statistical significance of difference at each time point between two genotypes. Student's *t* test or the Mann–Whitney *U* test was used for statistical analysis. $^{\#\#}P < 0.01$. *E*, relative Ca^{2+} responses in *rut*^{1}; MB-LexA LexAop-*GCaMP6f*/UAS-*rut*; R13F02-GAL4 /+ (black line; $n = 6$) and *rut*^{1}; MB-LexA LexAop-*GCaMP6f*/+; R13F02-GAL4 /+ (red line; $n = 6$). Hash symbols indicate the statistical significance of difference at each time point between two genotypes. Student's *t* test or the Mann–Whitney *U* test was used for statistical analysis. $^{\#}P < 0.05$. *F*, relative Ca^{2+} responses in *rut*^{1}; GH146/UAS-*rut*; MB-LexA LexAop-*GCaMP6m*/+ (black line; $n = 6$), and *rut*^{1}; GH146/+; MB-LexA LexAop-*GCaMP6m*/+ (red line; $n = 6$). No significant difference was detected at each point between two genotypes. Student's *t* test was used for statistical analysis. [Colour figure can be viewed at wileyonlinelibrary.com]

Pharmacology

To block the $GABA_A$ receptor or dopamine receptor, dissected brains were incubated in HL3 medium containing the blocker of each receptor (picrotoxin or butaclamol) or DMSO for 10 min before the start of recording. During the experiments, fresh HL3 medium containing the drug was infused every 5–10 min. To stimulate AC during repetitive AL stimulation, brains were incubated in HL3 medium containing 10 μM forskolin or DMSO for 10 min before repetitive AL stimulation. After the end of repetitive AL stimulation, 10 μM forskolin or DMSO was washed out.

Chemicals

Picrotoxin (cat. no. P1675), butaclamol ((+)-butaclamol hydrochloride; cat. no. D033) and forskolin (cat. no. F6886) were purchased from Sigma-Aldrich (St Louis, MO, USA). Picrotoxin, butaclamol and forskolin were dissolved in DMSO.

Statistical analysis

The Kolmogorov–Smirnov test was used to estimate whether the data were normally distributed. When the data were not distributed normally, we carried out the log transformation of the data. When the basic data or transformed data were normally distributed, Student's *t* test was used for pairwise comparison, and one-way ANOVA was carried out for multiple pairwise comparisons. When the transformed data were not distributed normally, the Mann–Whitney *U* test was used for pairwise comparisons, and non-parametric ANOVA (Kruskal–Wallis test) was used for multiple comparisons. The computer software IBM SPSS statistics 22 (IBM Japan, Ltd, Tokyo, Japan) or BellCurve for Excel (Social Survey Research Information Co., Ltd, Tokyo, Japan) was used for these tests.

Results

Repetitive AL stimulation reduces Ca^{2+} responses in MB neurons

To measure Ca^{2+} responses in adult MB neurons, we used the green fluorescent protein-based calcium indicator GCaMP3 (Tian *et al.* 2009). The GAL4/UAS binary gene expression system (Brand & Perrimon, 1993) was used for the targeted expression of GCaMP3 in the MB neurons (Fig. 1*A*). In an isolated cultured fly brain, electrical AL stimulation elicits robust Ca^{2+} responses in the tip of the MB α lobe via synaptic transmissions between PNs and MB neurons (Ueno *et al.* 2013). First, we measured AL-stimulation-induced Ca^{2+} responses in the α lobe tip after several stimulus trains, and examined whether repetitive AL stimulation induces synaptic plasticity (Fig. 1*A*). When the repetitive AL stimulation was less than 30 stimulus trains, the relative Ca^{2+} responses did not change or return to the baseline level immediately after the AL stimulation (Fig. 1*B*). However, when repetitive AL stimulation was more than 40 stimulus trains, the relative Ca^{2+} responses after the AL stimulation were significantly reduced in comparison with those before the AL stimulation, and the degree of the reduction of Ca^{2+} responses was dependent on the number of stimulus trains (Fig. 1*B*). In addition, the significant reduction of Ca^{2+} responses was consistently maintained for at least 30 min after AL stimulation with 40 stimulus trains (Fig. 1*C*). Since the AL stimulation-induced Ca^{2+} responses in horizontal lobes (β, β' and γ) were extremely weak and infrequent, as previously reported (Ueno *et al.* 2013), we next examined whether the reduction of Ca^{2+}

responses is detected in the α′ lobe. In contrast to the α lobe tip, we did not detect significant changes in the α′ lobe tip after repetitive AL stimulation with 40 trains (Fig. 1*D*). Thus, in all subsequent experiments, we applied AL stimulation with 40 stimulus trains to induce the reduction of MB Ca^{2+} responses.

Resistant to dieldrin, which encodes a $GABA_A$ receptor, is expressed in MB neurons (Harrison *et al.* 1996). When PNs are activated, MB neurons receive cholinergic inputs from PNs and GABAergic inputs from anterior paired lateral neurons (Lin *et al.* 2014). Thus, we next determined whether the AL stimulation-induced reduction of Ca^{2+}

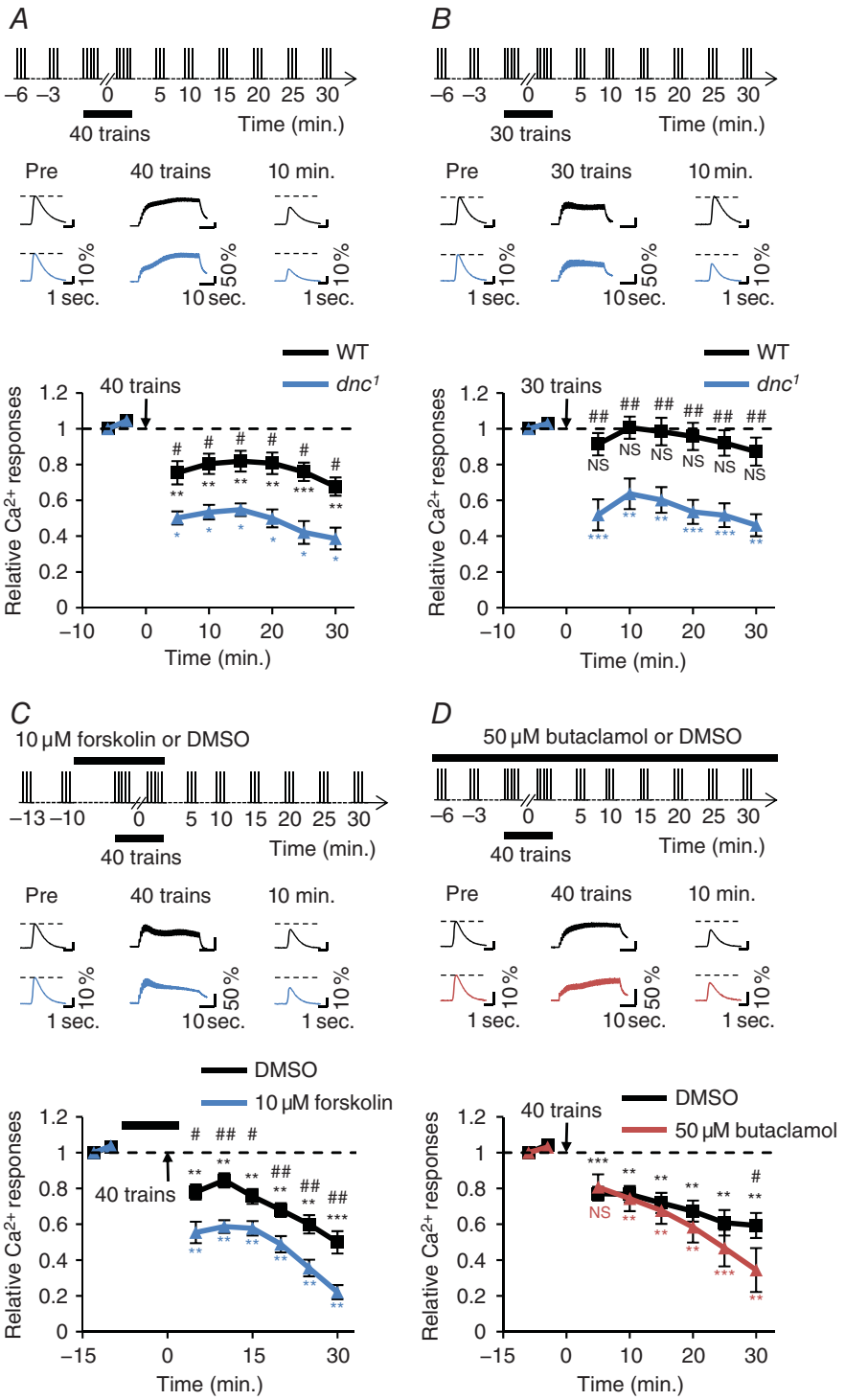

Figure 3. Increasing cAMP production enhances the reduction of Ca^{2+} responses

The upper panels show schematic diagrams of the stimulation protocol. Middle panels show typical Ca^{2+} responses in the α lobe tip 3 or 10 min before (Pre), during and 10 min after the application of 30 or 40 stimulus trains. Asterisks indicate the statistical significance of the difference between before and after the application of 30 or 40 stimulus trains. Student's *t* test or the Mann–Whitney *U* test was used for statistical analysis. Error bars represent SEM. NS, not significant; $^{*}P < 0.05$; $^{**}P < 0.01$; $^{***}P < 0.001$. *A*, the reduction of Ca^{2+} responses was enhanced in the *dnc*^{1} mutant (*dnc*^{1}; MB247 UAS-*GCaMP3*/+; $n = 4$; blue line) compared with the wild-type (+; MB247 UAS-*GCaMP3*/+; $n = 6$; black line). Hash symbols indicate the statistical significance of difference at each time point between the wild-type and *dnc*^{1}. The Mann–Whitney *U* test was used for statistical analysis. $^{\#}P < 0.05$. *B*, the reduction of Ca^{2+} responses was induced in the *dnc*^{1} mutant (*dnc*^{1}; MB247 UAS-*GCaMP3*/+; $n = 6$; blue line) by the application of 30 stimulus trains, while it was not induced in the wild-type (+; MB247 UAS-*GCaMP3*/+; $n = 6$; black line). Hash symbols indicate the statistical significance of difference at each time point between the wild-type and *dnc*^{1}. Student's *t* test or the Mann–Whitney *U* test was used for statistical analysis. $^{\#\#}P < 0.01$. *C*, the reduction of Ca^{2+} responses was enhanced by the treatment of the AC activator forskolin (blue line; $n = 7$) compared with that of DMSO as the control (black line; $n = 6$) in the wild-type (+; MB247 UAS-*GCaMP3*/+). The black rectangle indicates the time of forskolin or DMSO treatment. Hash symbols indicate the statistical significance of difference at each time point between forskolin treatment and DMSO treatment. Student's *t* test was used for statistical analysis. $^{\#}P < 0.05$; $^{\#\#}P < 0.01$. *D*, the reduction of Ca^{2+} responses was not suppressed by the treatment of the dopamine receptor blocker butaclamol (red line; $n = 6$) compared with that of DMSO as the control (black line; $n = 6$) in the wild-type (+; MB247 UAS-*GCaMP3*/+). The hash symbol indicates the statistical significance of the difference between butaclamol treatment and DMSO treatment. Student's *t* test was used for statistical analysis. $^{\#}P < 0.05$. [Colour figure can be viewed at wileyonlinelibrary.com]

responses results from the enhancement of inhibitory transmission via $GABA_A$ receptors on MB neurons. The $GABA_A$ receptor blocker picrotoxin was used in the experiments (Su & O'Dowd, 2003). It has been reported that picrotoxin treatment acutely enhances the AL stimulation-induced Ca^{2+} responses (Ueno *et al.* 2013). However, far from stopping the reduction of Ca^{2+} responses in the MB neurons, the reduction of Ca^{2+} responses was promoted during picrotoxin treatment (Fig. 1*E*). Thus, it is unlikely that the reduction of Ca^{2+} responses in MB neurons simply results from the enhancement of GABA transmission after AL stimulation. In a study by *ex vivo* Ca^{2+} imaging analysis, picrotoxin treatment enhances MB Ca^{2+} responses induced by AL stimulation (Ueno *et al.* 2013). Thus, the treatment increases Ca^{2+} influx into the MB neurons during repetitive AL stimulation. Although rigorous physiological mechanisms of the reduction of Ca^{2+} responses enhanced by picrotoxin are still unclarified, picrotoxin-induced elevation of $[Ca^{2+}]_i$ in the MB neurons during repetitive AL stimulation may cause the enhanced reduction of Ca^{2+} responses.

Rut-AC in the MB, but not in the PNs, is essential for the reduction of Ca^{2+} responses in MB neurons

To identify molecular components regulating the reduction of MB Ca^{2+} responses induced by AL stimulation, we focused on cAMP signalling. *Drosophila rut*, which is mainly expressed in MB neurons, encodes Ca^{2+}/calmodulin-responsive AC (Levin *et al.* 1992). *rut*^{1} mutant flies with a loss-of-function mutation of *rut* were used in the experiments. *rut*^{1} showed almost no reduction of Ca^{2+} responses in the MB neurons (Fig. 2*A* and *B*). We next examined whether the induction of wild-type *rut* expression in a *rut* mutant background rescues the reduction of MB Ca^{2+} responses. In Fig. 2*D* and *E*, the GAL4/UAS system was used for wild-type *rut* transgene expression in the MB neurons of *rut*^{1}, and the LexA/LexAop system (Lai & Lee, 2006) was used for the targeted expression of the Ca^{2+} indicator GCaMP6m (Chen *et al.* 2013) in the MB neurons. Two MB-GAL4 lines (c772 and R13F02) were used in the experiments. Although GAL4 and UAS control flies with *rut*^{1} mutation exhibited the *rut*^{1} mutant phenotype (Fig. 2*C*, *D* and *E*, red lines), wild-type *rut* transgene expression in the MB neurons of *rut*^{1} rescued the *rut*^{1} mutant phenotype (Fig. 2*D* and *E*, black lines). In contrast to *rut* expression in the MB neurons, the targeted expression of the wild-type *rut* transgene in PNs could not rescue the *rut*^{1} mutant phenotype (Fig. 2*F*, black line), suggesting that Rut-AC-dependent cAMP production in the MB neurons, but not in the PNs, is critically involved in the reduction of MB Ca^{2+} responses after repetitive AL stimulation.

Forskolin treatment or *dnc*^{1} mutation promotes the reduction of Ca^{2+} responses after repetitive AL stimulation

In MB neurons, *dnc*, which encodes a phosphodiesterase, is also expressed (Davis, 2005). It is considered that cAMP level increases in *dnc*^{1} mutant flies with a hypomorphic mutation of *dnc* compared with wild-type flies (Byers *et al.* 1981). In contrast to *rut*^{1} mutation, *dnc*^{1} mutation enhanced the reduction of Ca^{2+} responses compared with the wild-type flies (Fig. 3*A*). Furthermore, although the repetitive AL stimulation with 30 stimulus trains was not sufficient to reduce the MB Ca^{2+} responses in wild-type flies (Fig. 1*B*), it induced the reduction of MB Ca^{2+} responses in *dnc*^{1} (Fig. 3*B*). Next, to increase cAMP

level transiently, we performed pharmacological treatment using an AC activator, forskolin (Boto *et al.* 2014). As was observed in dnc^1, forskolin treatment during repetitive AL stimulation also enhanced the reduction of Ca^{2+} responses in MB neurons (Fig. 3*C*). Thus, these findings show that the increase in cAMP level promotes the reduction of MB Ca^{2+} responses.

In *Drosophila*, four genes that encode dopamine receptors are identified (*Dop1R1*, *Dop1R2*, *Dop2R* and *DopEcR*), and these receptors are expressed in MB neurons (Crocker *et al.* 2016). Thus, cAMP could be produced by repetitive AL stimulation through the dopamine signalling pathway. To evaluate this possibility, we used a non-selective dopamine receptor blocker, butaclamol (Sugamori *et al.* 1995). However, butaclamol treatment hardly affected the reduction of Ca^{2+} responses in MB neurons (Fig. 3*D*). Thus, the reduction of MB Ca^{2+} responses may be independent of dopaminergic inputs.

The reduction of Ca^{2+} responses after repetitive AL stimulation is also detected in the MB calyx

Rut-AC is localized in the axonal lobes and dendritic calyx in the MB (Han *et al.* 1992), and cAMP signalling regulates Ca^{2+} responsivity in these regions (Pavot *et al.* 2015). To examine whether repetitive AL stimulation also induces the reduction of Ca^{2+} responses in the calyx, we observed AL stimulation-induced Ca^{2+} responses in the α lobe and calyx in the same brains (Figs 4*A* and 5*A*). After AL stimulation with 40 stimulus trains, Ca^{2+} responses in the calyx of wild-type flies were reduced, as was observed in the α lobe (Fig. 4*B* and *C*).

In contrast to wild-type flies, rut^1 flies showed impaired reduction of Ca^{2+} responses in the calyx (Fig. 5*B*). However, the targeted expression of the wild-type *rut* transgene in the MB neurons in rut^1 mutant flies (rut^1; c772/UAS-*rut*) induced the reduction of Ca^{2+} responses

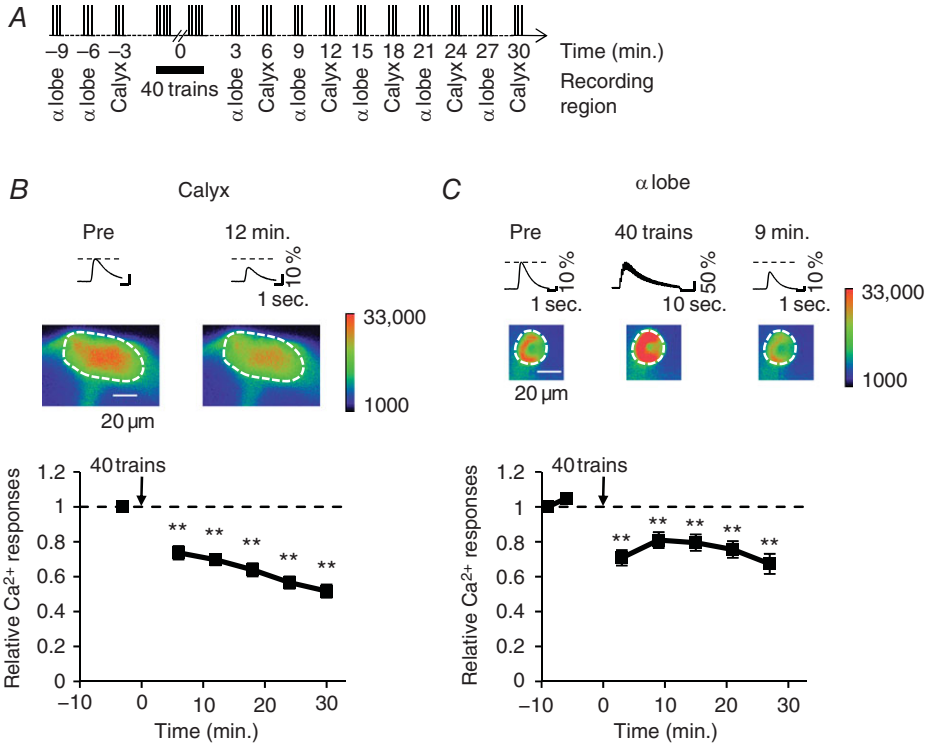

Figure 4. Repetitive AL stimulation induces the reduction of Ca^{2+} responses in the MB calyx
A, schematic diagrams of AL stimulation protocol. AL stimulation was applied sequentially every 3 min before and after repetitive AL stimulation with 40 trains. Ca^{2+} responses were recorded in the α lobe and calyx in the same brain. *B* and *C*, +; MB247 UAS-*GCaMP3*/+ males were used in the experiments. Asterisks indicate the statistical significance of the difference between before and after the application of 40 stimulus trains. The Mann–Whitney *U* test was used for statistical analysis. Error bars represent SEM. $^{**}P < 0.01$; $n = 7$. *B*, Ca^{2+} responses in the calyx after repetitive AL stimulation. The upper panel shows typical Ca^{2+} responses in the calyx 3 min before (Pre) and 12 min after the application of 40 stimulus trains. Pseudo-color represents the intensity of GCaMP3 fluorescence. The area enclosed by a dashed circle is the calyx. *C*, Ca^{2+} responses in the α lobe after repetitive AL stimulation in the same brain shown in *B*. The upper panel shows typical Ca^{2+} responses in the α lobe 6 min before (Pre), during and 9 min after the application of 40 stimulus trains. The area enclosed by dashed lines is the α lobe. [Colour figure can be viewed at wileyonlinelibrary.com]

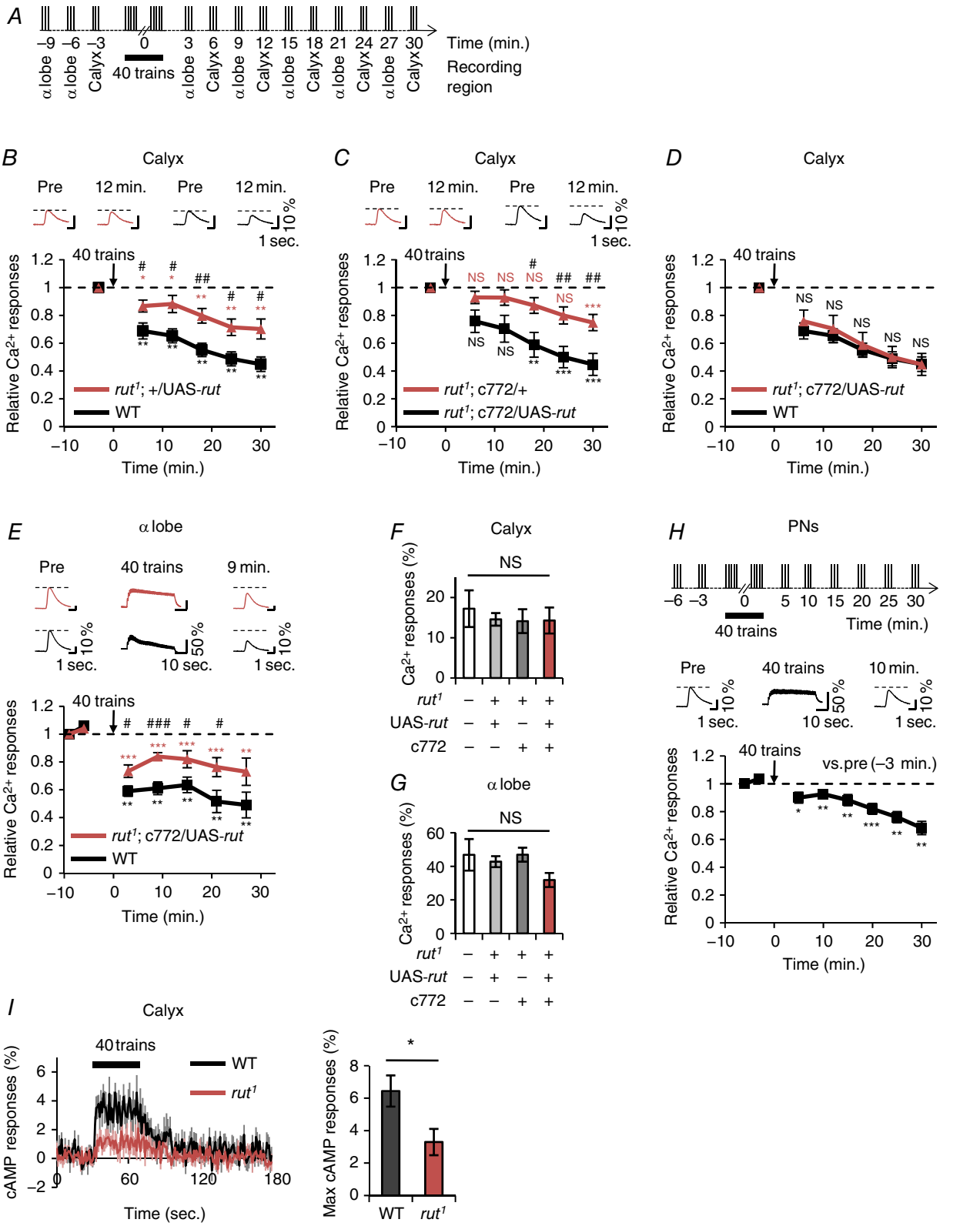

Figure 5. *rut* expression in MB neurons is required for the reduction of Ca^{2+} responses in the MB calyx

A, schematic diagram of AL stimulation protocol. *B* and *C*, the upper panels show typical Ca^{2+} responses in the calyx 3 min before (Pre) and 12 min after the application of 40 stimulus trains. *E*, the upper panels show typical Ca^{2+} responses in the α lobe 6 min before (Pre), during and 9 min after the application of 40 stimulus trains. *B*, *C* and *E*, asterisks indicate the statistical significance of the difference between before and after the application of 40 stimulus trains. The Mann–Whitney *U* test was used for statistical analysis. Error bars represent SEM. NS, not significant; $^{*}P < 0.05$; $^{**}P < 0.01$; $^{***}P < 0.001$. *B*, relative Ca^{2+} responses in the calyx of wild-type (black line; +; +; MB-LexA LexAop-*GCaMP6m*/+; $n = 7$) and *rut*^{1} (red line; *rut*^{1}; +/UAS-*rut*; MB-LexA LexAop-*GCaMP6m*/+; $n = 7$). Hash symbols indicate the statistical significance of difference at each time point between two genotypes. Student's *t* test or the Mann–Whitney *U* test was used for statistical analysis.$^{\#}P < 0.05$; $^{\#\#}P < 0.01$. *C*, relative Ca^{2+} responses in the calyx of *rut*^{1}; c772/UAS-*rut*; MB-LexA LexAop-*GCaMP6m*/+ (black line; $n = 9$) and *rut*^{1}; c772/+; MB-LexA LexAop-*GCaMP6m*/+ (red line; $n = 9$). Hash symbols indicate the statistical significance of difference at each time point between two genotypes. Student's *t* test was used for statistical analysis. $^{\#}P < 0.05$; $^{\#\#}P < 0.01$. *D*, no significant difference was detected at each time point between the wild-type (black line; +; +; MB-LexA LexAop-*GCaMP6m*/+) and *rut*^{1}; c772/UAS-*rut* (red line; *rut*^{1}; c772/UAS-*rut*; MB-LexA LexAop-*GCaMP6m*/+) in the calyx. The results for the wild-type are the same as those shown in *B*, and the results for *rut*^{1}; c772/UAS-*rut* are the same as those shown in *C*. The Mann–Whitney *U* test was used for statistical analysis. Error bars represent SEM. NS, not significant. *E*, in the α lobe, the degree of reduction of Ca^{2+} responses in *rut*^{1}; c772/UAS-*rut* (red line; *rut*^{1}; c772/UAS-*rut*; MB-LexA LexAop-*GCaMP6m*/+) was lower than that in the wild-type (black line; +; +; MB-LexA LexAop-*GCaMP6m*/+). Hash symbols indicate the statistical significance of difference at each time point between two genotypes. Student's *t* test was used for statistical analysis. Error bars represent SEM. $^{\#}P < 0.05$; $^{\#\#\#}P < 0.001$. *F* and *G*, Ca^{2+} responses to AL stimulation with a stimulus train in the calyx (*F*) and the α lobe (*G*). +; +; MB-LexA LexAop-*GCaMP6m*/+ (white bar), *rut*^{1}; +/UAS-*rut*; MB-LexA LexAop-*GCaMP6m*/+ (light grey bar), *rut*^{1}; c772/+; MB-LexA LexAop-*GCaMP6m*/+ (grey bar), and *rut*^{1}; c772/UAS-*rut*; MB-LexA LexAop-*GCaMP6m*/+ (red bar) were used for analysis. One-way ANOVA or the non-parametric ANOVA (Kruskal–Wallis test) was used for statistical analysis. Error bars represent SEM. NS, not significant. *H*, +; GH146 UAS-*GCaMP6m*/+; + males were used. Ca^{2+} responses before and after application of 40 stimulus trains in the terminal of PNs. The upper panel shows a schematic diagram of the stimulation protocol. The middle panel shows typical Ca^{2+} responses in the terminal of PNs 3 min before (Pre), during and 10 min after the application of 40 stimulus trains. Asterisks indicate the statistical significance of difference at each time point between before and after the application of 40 stimulus trains. Student's *t* test or the Mann–Whitney *U* test was used for statistical analysis. Error bars represent SEM. $^{*}P < 0.05$; $^{**}P < 0.01$; $^{***}P < 0.001$; $n = 6$. *I*, cAMP responses during repetitive AL stimulation in the wild-type (+; +; 30Y UAS-*Epac1-camps*/+) and *rut*^{1} (*rut*^{1}; +; 30Y UAS-*Epac1-camps*/+). Time course of cAMP responses in the MB calyx (left) and summary of maximum scores from each trace (right). The black line and bar indicate results for the wild-type (WT; $n = 7$) and the red line and bar indicate those for *rut*^{1} ($n = 7$). The black rectangle indicates the time of repetitive AL stimulation. Student's *t* test was used for pairwise comparisons. Error bars represent SEM. $^{*}P < 0.05$. [Colour figure can be viewed at wileyonlinelibrary.com]

after repetitive AL stimulation in the calyx (Fig. 5*C*). Regarding the degree of reduction of Ca^{2+} responses in the calyx, no significant differences were detected between the wild-type and *rut*^{1}; c772/UAS-*rut* flies (Fig. 5*D*), indicating that *rut* expression in MB neurons in *rut*^{1} completely rescues the *rut*^{1} phenotype in the calyx. In the α lobe, the degree of reduction of Ca^{2+} responses in *rut*^{1}; c772/UAS-*rut* flies was lower than that in wild-type flies (Fig. 5*E*). Thus, these findings indicate that *rut* expression in *rut*^{1} partially rescues the *rut*^{1} phenotype in the α lobe.

It is possible that the impaired reduction of Ca^{2+} responses in the *rut*^{1} mutant calyx or α lobe results from reduced Ca^{2+} responses to AL stimulation. Thus, Ca^{2+} responses to AL stimulation with one stimulus train, that is, without repetitive AL stimulation, were compared among four genotypes (Fig. 5*F* and *G*). In the calyx and α lobe, no significant differences were detected in Ca^{2+} responses (Fig. 5*F* and *G*). Thus, it is unlikely that the reduced Ca^{2+} responses to electrical stimulation of AL in *rut*^{1} impair the reduction of Ca^{2+} responses after repetitive AL stimulation.

Next, we examined whether the activity of PNs is modified after repetitive AL stimulation with 40 stimulus trains. AL stimulation slightly reduced Ca^{2+} responses in PN axon terminals after repetitive AL stimulation (Fig. 5*H*), suggesting that repetitive AL stimulation slightly modifies physiological properties of PN axon terminals. However, the reduction of Ca^{2+} responses in axon terminals in PNs was smaller in magnitude than that in the MB calyx (Fig. 5*B* and *H*). Furthermore, the impaired reduction of Ca^{2+} responses in MB neurons in *rut*^{1} flies was fully rescued by the expression of the wild-type *rut* transgene in the calyx in *rut*^{1} (Fig. 5*D*). Thus, it is most unlikely that the cAMP-dependent reduction of Ca^{2+} responses in the calyx simply results from the physiological properties of PNs modified by the repetitive AL stimulation.

If Rut-AC-dependent cAMP production is required for the reduction of Ca^{2+} responses in the calyx, AL stimulation with 40 stimulus trains should increase the cAMP level in the calyx. We measured the cAMP level in the calyx using a FRET-based cAMP indicator, Epac1-camps (Nikolaev *et al.* 2004). Although the cAMP level increased in the wild-type calyx during repetitive AL stimulation, cAMP production was inhibited in *rut*^{1} mutant flies (Fig. 5*I*).

Discussion

In this study, we found novel non-associative synaptic depression in the MB calyx of an isolated cultured *Drosophila* brain. Ca^{2+} responses in the calyx were reduced after repetitive AL stimulation (Fig. 4), and *rut* expression in the MB neurons was essential for the reduction of Ca^{2+} responses in the calyx (Fig. 5). Since Rut-AC is a Ca^{2+}/calmodulin-dependent AC (Levin *et al.* 1992), it is possible that Rut-AC-dependent cAMP production was induced via the increase in $[Ca^{2+}]_i$. AL–MB synaptic transmissions are cholinergic and

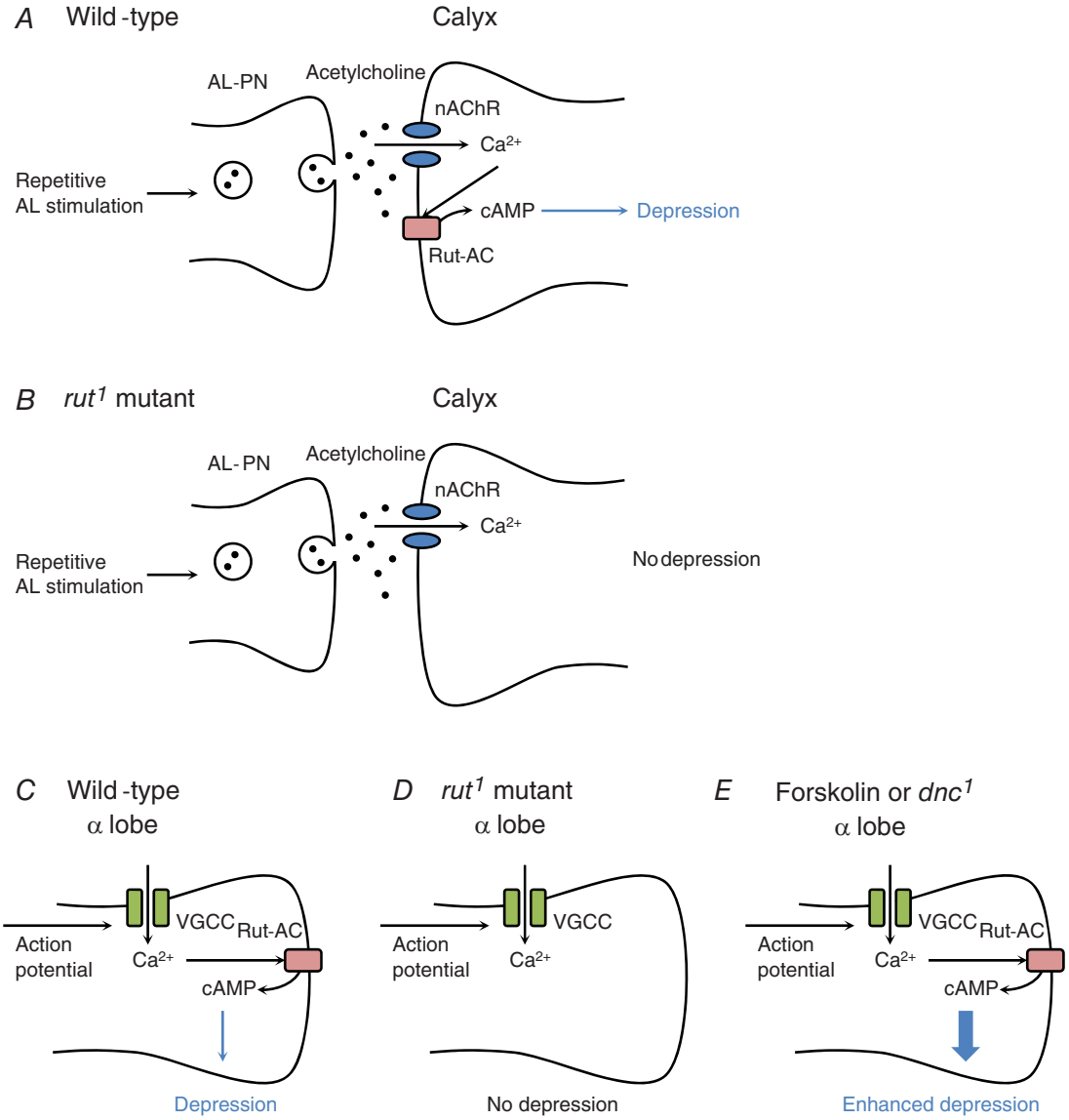

Figure 6. Possible model of the reduction of Ca^{2+} responses in the MB calyx and α lobe
A, in the wild-type, the projection neurons of the antennal lobe (AL-PN) release acetylcholine (black dots) following repetitive AL stimulation, and nAChRs (blue) are activated in the MB calyx. The increase in $[Ca^{2+}]_i$ through nAChRs stimulates Rut-AC (red), and cAMP is produced. The increase in cAMP level induces synaptic depression in the MB calyx. *B*, in the *rut*^{1} mutant, repetitive AL stimulation induces Ca^{2+} entry through nAChRs. However, Rut-AC-dependent cAMP production does not occur. Thus, synaptic depression also does not occur. *C*, in the wild-type, action potentials generated by repetitive AL stimulation may induce Ca^{2+} influx through voltage-gated calcium channels (VGCCs; green) in the α lobe. The increase in $[Ca^{2+}]_i$ activates Rut-AC, and cAMP is produced. The increase in cAMP level induces the reduction of Ca^{2+} responses in the α lobe. *D*, in the *rut*^{1} mutant, repetitive AL stimulation induces Ca^{2+} influx into the α lobe. However, Rut-AC-dependent cAMP production does not occur. Thus, the reduction of Ca^{2+} responses also does not occur. *E*, forskolin treatment or *dnc*^{1} mutation increases the cAMP level. In this situation, the reduction of Ca^{2+} responses in the α lobe is promoted. [Colour figure can be viewed at wileyonlinelibrary.com]

nicotinic acetylcholine receptors (nAChRs) are expressed in the calyx (Fayyazuddin *et al.* 2006). Thus, it is likely that increasing $[Ca^{2+}]_i$ through nAChRs activates Rut-AC. Taken together, the synaptic plasticity in the calyx may be explained as follows. In the wild-type flies, the cAMP level through nAChRs increases in the calyx during repetitive AL stimulation, and the increased cAMP level induces synaptic depression in the calyx (Fig. 6*A*). However, in rut^1, Rut-AC-dependent cAMP production is inhibited during repetitive AL stimulation; consequently, synaptic depression does not occur in the calyx (Fig. 6*B*). In rut^1 mutant flies, cAMP production was inhibited, whereas it was slightly detected during repetitive AL stimulation (Fig. 5*I*). Since four AC genes apart from *rut* are highly expressed in the adult brain (Naganos *et al.* 2016), these ACs in MB neurons may contribute to the slight increase in cAMP level in rut^1. However, rut^1 did not reduce Ca^{2+} responses after repetitive AL stimulation (Fig. 5), suggesting that Rut-AC-dependent cAMP production in the calyx is sufficient for the reduction of Ca^{2+} responses after repetitive AL stimulation.

We further found that Ca^{2+} responses in the α lobe were also reduced after repetitive AL stimulation (Fig. 1). The reduction rate was dependent on the number of stimulus trains (Fig. 1). As was observed in the calyx, *rut* expression in MB neurons was required for the reduction of Ca^{2+} responses in the α lobe (Fig. 5). In contrast to the rut^1 mutation, the dnc^1 mutation or forskolin treatment promoted the reduction of Ca^{2+} responses after repetitive AL stimulation with 40 stimulus trains (Fig. 3*A* and *C*). In addition, the repetitive AL stimulation with 30 stimulus trains was sufficient to reduce the MB Ca^{2+} responses in dnc^1 (Fig. 3*B*). Taking these results together, in wild-type flies, the increase in Rut-AC-dependent cAMP production during repetitive AL stimulation induces the reduction of Ca^{2+} responses in the α lobe (Fig. 6*C*). However, in rut^1, the cAMP production is inhibited during repetitive AL stimulation; consequently, the Ca^{2+} responses are not reduced in the α lobe (Fig. 6*D*). In contrast, forskolin treatment or dnc^1 mutation further increases the cAMP level during repetitive AL stimulation. Thus, the reduction of Ca^{2+} responses is also promoted in the α lobe (Fig. 6*E*).

In this study, we identified that repetitive AL stimulation induces the reduction of Ca^{2+} responses in the calyx and α lobe. The *rut* expression in MB neurons in rut^1 completely rescued the rut^1 phenotype in the calyx (Fig. 5*D*). However, in the α lobe, the *rut* expression partially rescued the rut^1 phenotype (Fig. 5*E*), suggesting that Rut-AC in brain neurons other than MBs also contributes to the reduction of Ca^{2+} responses in the α lobe. Thus, although the detailed clarification of the physiological mechanisms regulating the reduction of Ca^{2+} responses in the α lobe remains elusive, it is possible that the reduction of Ca^{2+} responses in the α lobe does not simply result from the altered Ca^{2+} responsivity in the calyx.

We previously reported that AL stimulation with 12 stimulus trains (intertrain intervals of 5 s) alone does not induce plasticity at AL–MB synapses in the dissected brain, whereas simultaneous associative stimulation of the AL (12 stimulus trains) and AFV generates long-term enhancement (Ueno *et al.* 2013). In this study, we showed that AL stimulation with more than 40 stimulus trains (intertrain intervals of 1 s) induces synaptic depression, suggesting that AL stimulation with 12 stimulus trains is insufficient for producing cAMP in the MB calyx, which is essential for synaptic depression. In honeybee, MB responses gradually increase during continuous low-frequency stimulation of AL (0.1 ms pulse duration, interpulse intervals of 1–50 s), indicating that MB neurons represent sensitization through AL–MB synaptic transmission (Oleskevich *et al.* 1997). Since the stimulation protocol of AL in the previous study is completely different from that in this study, in insects, the generation of non-associative sensitization or depression at AL–MB synapses may be dependent on the protocol of AL stimulation.

Insects show species-specific behavioural modification following odour exposure (Anderson *et al.* 2003; Minoli *et al.* 2013). Similarly to other insect species, *Drosophila* also shows odour-based behavioural plasticity. Prolonged odour exposure leads to reduced behavioural responses, and this behavioural plasticity is considered to be caused by experience-dependent or adaptive synaptic plasticity in the AL (Sachse *et al.* 2007; Das *et al.* 2011; Pech *et al.* 2015). In addition, MB neurons also play an important role in the regulation of odour-based behavioural plasticity. The locomotor activity of adult flies rapidly and transiently increases following exposure to ethanol vapour, and this odour-mediated startle response is attenuated by repetitive exposure to ethanol vapour (Cho *et al.* 2004). However, dysfunction of MB neurons and *rut* mutations reduce this non-associative behavioural plasticity (Cho *et al.* 2004), suggesting that the cAMP signalling pathway in the MB neurons regulate non-associative behavioural plasticity induced by olfactory inputs. In this study, we showed by *ex vivo* imaging analysis that repetitive AL stimulation induces synaptic depression in the MB calyx. Although the role of synaptic depression *in vivo* still remains unclarified, it is likely that the synaptic depression in the MB calyx also causes odour-based behavioural plasticity. As was observed in *Drosophila*, in the honey bee *Apis mellifera carnica*, AL–MB transmission is also cholinergic (Goldberg *et al.* 1999), and odour-evoked Ca^{2+} responses in the MB calyx are attenuated after repeated odour stimulation (Szyszka *et al.* 2008). Thus, it is possible that the non-associative olfactory learning based on synaptic depression in the MB calyx is evolutionarily conserved among insect species. *Ex vivo* imaging to monitor synaptic depression in the MB calyx will be carried out to identify additional molecules or clarify the physiological property

underlying odour-based behavioural plasticity in insect species.

References

Abel T & Nguyen PV (2008). Regulation of hippocampus-dependent memory by cyclic AMP-dependent protein kinase. *Prog Brain Res* **169**, 97–115.

Anderson P, Sadek MM & Hansson BS (2003). Pre-exposure modulates attraction to sex pheromone in a moth. *Chem Senses* **28**, 285–291.

Aso Y, Hattori D, Yu Y, Johnston RM, Iyer NA, Ngo TT, Dionne H, Abbott LF, Axel R, Tanimoto H & Rubin GM (2014). The neuronal architecture of the mushroom body provides a logic for associative learning. *Elife* **3**, e04577.

Boto T, Louis T, Jindachomthong K, Jalink K & Tomchik SM (2014). Dopaminergic modulation of cAMP drives nonlinear plasticity across the *Drosophila* mushroom body lobes. *Curr Biol* **24**, 822–831.

Brand AH & Perrimon N (1993). Targeted gene expression as a means of altering cell fates and generating dominant phenotypes. *Development* **118**, 401–415.

Byers D, Davis RL & Kiger JA Jr (1981). Defect in cyclic AMP phosphodiesterase due to the *dunce* mutation of learning in *Drosophila melanogaster*. *Nature* **289**, 79–81.

Chen TW, Wardill TJ, Sun Y, Pulver SR, Renninger SL, Baohan A, Schreiter ER, Kerr RA, Orger MB, Jayaraman V, Looger LL, Svoboda K & Kim DS (2013). Ultrasensitive fluorescent proteins for imaging neuronal activity. *Nature* **499**, 295–300.

Cho W, Heberlein U & Wolf FW (2004). Habituation of an odorant-induced startle response in *Drosophila*. *Genes Brain Behav* **3**, 127–137.

Cohn R, Morantte I & Ruta V (2015). Coordinated and compartmentalized neuromodulation shapes sensory processing in *Drosophila*. *Cell* **163**, 1742–1755.

Collingridge GL, Peineau S, Howland JG & Wang YT (2010). Long-term depression in the CNS. *Nat Rev Neurosci* **11**, 459–473.

Crittenden JR, Skoulakis EM, Han KA, Kalderon D & Davis RL (1998). Tripartite mushroom body architecture revealed by antigenic markers. *Learn Mem* **5**, 38–51.

Crocker A, Guan XJ, Murphy CT & Murthy M (2016). Cell-type-specific transcriptome analysis in the *Drosophila* mushroom body reveals memory-related changes in gene expression. *Cell Rep* **15**, 1580–1596.

Das S, Sadanandappa MK, Dervan A, Larkin A, Lee JA, Sudhakaran IP, Priya R, Heidari R, Holohan EE, Pimentel A, Gandhi A, Ito K, Sanyal S, Wang JW, Rodrigues V & Ramaswami M (2011). Plasticity of local GABAergic interneurons drives olfactory habituation. *Proc Natl Acad Sci U S A* **108**, E646–654.

Davis RL (2005). Olfactory memory formation in *Drosophila*: from molecular to systems neuroscience. *Annu Rev Neurosci* **28**, 275–302.

Davis RL (2011). Traces of *Drosophila* memory. *Neuron* **70**, 8–19.

Fayyazuddin A, Zaheer MA, Hiesinger PR & Bellen HJ (2006). The nicotinic acetylcholine receptor Dα7 is required for an escape behavior in *Drosophila*. *PLoS Biol* **4**, e63.

Glanzman DL (2009). Habituation in *Aplysia*: the Cheshire cat of neurobiology. *Neurobiol Learn Mem* **92**, 147–154.

Goldberg F, Grunewald B, Rosenboom H & Menzel R (1999). Nicotinic acetylcholine currents of cultured Kenyon cells from the mushroom bodies of the honey bee *Apis mellifera*. *J Physiol* **514**, 759–768.

Guo HF & Zhong Y (2006). Requirement of Akt to mediate long-term synaptic depression in *Drosophila*. *J Neurosci* **26**, 4004–4014.

Han PL, Levin LR, Reed RR & Davis RL (1992). Preferential expression of the *Drosophila rutabaga* gene in mushroom bodies, neural centers for learning in insects. *Neuron* **9**, 619–627.

Harrison JB, Chen HH, Sattelle E, Barker PJ, Huskisson NS, Rauh JJ, Bai D & Sattelle DB (1996). Immunocytochemical mapping of a C-terminus anti-peptide antibody to the GABA receptor subunit, RDL in the nervous system in *Drosophila melanogaster*. *Cell Tissue Res* **284**, 269–278.

Hawkins RD, Kandel ER & Bailey CH (2006). Molecular mechanisms of memory storage in *Aplysia*. *Biol Bull* **210**, 174–191.

Heisenberg M (2003). Mushroom body memoir: from maps to models. *Nat Rev Neurosci* **4**, 266–275.

Hige T, Aso Y, Modi MN, Rubin GM & Turner GC (2015). Heterosynaptic plasticity underlies aversive olfactory learning in *Drosophila*. *Neuron* **88**, 985–998.

Ho VM, Lee JA & Martin KC (2011). The cell biology of synaptic plasticity. *Science* **334**, 623–628.

Kandel ER (2001). The molecular biology of memory storage: a dialogue between genes and synapses. *Science* **294**, 1030–1038.

Kandel ER (2012). The molecular biology of memory: cAMP, PKA, CRE, CREB-1, CREB-2, and CPEB. *Mol Brain* **5**, 14.

Korte M & Schmitz D (2016). Cellular and system biology of memory: timing, molecules, and beyond. *Physiol Rev* **96**, 647–693.

Lai SL & Lee T (2006). Genetic mosaic with dual binary transcriptional systems in *Drosophila*. *Nat Neurosci* **9**, 703–709.

Levin LR, Han PL, Hwang PM, Feinstein PG, Davis RL & Reed RR (1992). The *Drosophila* learning and memory gene *rutabaga* encodes a Ca^{2+}/calmodulin-responsive adenylyl cyclase. *Cell* **68**, 479–489.

Lin AC, Bygrave AM, de Calignon A, Lee T & Miesenbock G (2014). Sparse, decorrelated odor coding in the mushroom body enhances learned odor discrimination. *Nat Neurosci* **17**, 559–568.

Minoli S, Palottini F & Manrique G (2013). The main component of an alarm pheromone of kissing bugs plays multiple roles in the cognitive modulation of the escape response. *Front Behav Neurosci* **7**, 77.

Naganos S, Ueno K, Horiuchi J & Saitoe M (2016). Learning defects in *Drosophila* growth restricted *chico* mutants are caused by attenuated adenylyl cyclase activity. *Mol Brain* **9**, 37.

Nicoll RA (2017). A brief history of long-term potentiation. *Neuron* **93**, 281–290.

Nikolaev VO, Bunemann M, Hein L, Hannawacker A & Lohse MJ (2004). Novel single chain cAMP sensors for receptor-induced signal propagation. *J Biol Chem* **279**, 37215–37218.

Oleskevich S, Clements JD & Srinivasan MV (1997). Long-term synaptic plasticity in the honeybee. *J Neurophysiol* **78**, 528–532.

Pavot P, Carbognin E & Martin JR (2015). PKA and cAMP/CNG channels independently regulate the cholinergic Ca^{2+}-response of *Drosophila* mushroom body neurons. *eNeuro* **2**, ENEURO.0054-14.2015.

Pech U, Revelo NH, Seitz KJ, Rizzoli SO & Fiala A (2015). Optical dissection of experience-dependent pre- and postsynaptic plasticity in the *Drosophila* brain. *Cell Rep* **10**, 2083–2095.

Sachse S, Rueckert E, Keller A, Okada R, Tanaka NK, Ito K & Vosshall LB (2007). Activity-dependent plasticity in an olfactory circuit. *Neuron* **56**, 838–850.

Stewart BA, Atwood HL, Renger JJ, Wang J & Wu CF (1994). Improved stability of *Drosophila* larval neuromuscular preparations in haemolymph-like physiological solutions. *J Comp Physiol A* **175**, 179–191.

Su H & O'Dowd DK (2003). Fast synaptic currents in *Drosophila* mushroom body Kenyon cells are mediated by α-bungarotoxin-sensitive nicotinic acetylcholine receptors and picrotoxin-sensitive GABA receptors. *J Neurosci* **23**, 9246–9253.

Sugamori KS, Demchyshyn LL, McConkey F, Forte MA & Niznik HB (1995). A primordial dopamine D1-like adenylyl cyclase-linked receptor from *Drosophila melanogaster* displaying poor affinity for benzazepines. *FEBS Lett* **362**, 131–138.

Szyszka P, Galkin A & Menzel R (2008). Associative and non-associative plasticity in Kenyon cells of the honeybee mushroom body. *Front Syst Neurosci* **2**, 3.

Tian L, Hires SA, Mao T, Huber D, Chiappe ME, Chalasani SH, Petreanu L, Akerboom J, McKinney SA, Schreiter ER, Bargmann CI, Jayaraman V, Svoboda K & Looger LL (2009). Imaging neural activity in worms, flies and mice with improved GCaMP calcium indicators. *Nat Methods* **6**, 875–881.

Ueno K, Naganos S, Hirano Y, Horiuchi J & Saitoe M (2013). Long-term enhancement of synaptic transmission between antennal lobe and mushroom body in cultured *Drosophila* brain. *J Physiol* **591**, 287–302.

Ueno K, Suzuki E, Naganos S, Ofusa K, Horiuchi J & Saitoe M (2017). Coincident postsynaptic activity gates presynaptic dopamine release to induce plasticity in *Drosophila* mushroom bodies. *Elife* **6**, e21076.

Vosshall LB & Stocker RF (2007). Molecular architecture of smell and taste in *Drosophila*. *Annu Rev Neurosci* **30**, 505–533.

Wang Y, Mamiya A, Chiang AS & Zhong Y (2008). Imaging of an early memory trace in the *Drosophila* mushroom body. *J Neurosci* **28**, 4368–4376.

Additional information

Competing interests

None declared.

Author contributions

S.S. and T.S. contributed to the conception or design of the work. S.S. performed most of the experiments. K.U. and M.S. contributed to the imaging study. T.S. supervised and wrote the manuscript with S.S., K.U. and M.S. All experiments were carried out in TMU and TMIMS. All authors have approved the final version of the manuscript and agree to be accountable for all aspects of the work. All persons designated as authors qualify for authorship, and all those who qualify for authorship are listed.

Funding

This work was supported by grants from JSPS KAKENHI (12J06931 to S.S., JP21700376 to K.U., 16H04816 and JP25650116 to T.S.) and the Ministry of Education, Culture, Sports, Science and Technology (JP25115006 to M.S., JP21115514 and JP23115714 to T.S.)

Acknowledgements

We thank S. Miyata for technical assistance. We also thank T. Miyashita and S. Naganos for helpful discussions.